

A coupled piezoelectric–electromagnetic energy harvesting technique for achieving increased power output through damping matching

Vinod R Challa, M G Prasad and Frank T Fisher

Department of Mechanical Engineering, Stevens Institute of Technology, Hoboken, NJ 07030, USA

E-mail: vchalla@stevens.edu and ffisher@stevens.edu

Received 16 February 2009, in final form 14 June 2009

Published 6 August 2009

Online at stacks.iop.org/SMS/18/095029

Abstract

Vibration energy harvesting is being pursued as a means to power wireless sensors and ultra-low power autonomous devices. From a design standpoint, matching the electrical damping induced by the energy harvesting mechanism to the mechanical damping in the system is necessary for maximum efficiency. In this work two independent energy harvesting techniques are coupled to provide higher electrical damping within the system. Here the coupled energy harvesting device consists of a primary piezoelectric energy harvesting device to which an electromagnetic component is added to better match the total electrical damping to the mechanical damping in the system. The first coupled device has a resonance frequency of 21.6 Hz and generates a peak power output of $\sim 332 \mu\text{W}$, compared to 257 and 244 μW obtained from the optimized, stand-alone piezoelectric and electromagnetic energy harvesting devices, respectively, resulting in a 30% increase in power output. A theoretical model has been developed which closely agrees with the experimental results. A second coupled device, which utilizes the d_{33} piezoelectric mode, shows a 65% increase in power output in comparison to the corresponding stand-alone, single harvesting mode devices. This work illustrates the design considerations and limitations that one must consider to enhance device performance through the coupling of multiple harvesting mechanisms within a single energy harvesting device.

(Some figures in this article are in colour only in the electronic version)

1. Introduction

Wireless sensors are becoming increasingly popular because of their wide potential application and ability to be employed in inaccessible and hostile environments. To realize the full potential of wireless sensors requires a self-sustainable power source, and vibration energy harvesting provides a promising solution in this regard. In addition, many other applications that consume low levels of energy could potentially be powered using mechanical vibrations. For example, portable and wireless devices (cell phones, mp3 players, etc) would benefit from longer battery life and the need for less frequent recharging, which could be accomplished by supplementing (or perhaps eventually fully replacing) existing batteries with

power harvested from vibration sources in the environment. However, in order to effectively power and/or recharge these wireless electronic devices using vibration energy, the effective power density and the total power output of the energy harvesting devices must be increased. While significant research has been conducted to enhance the vibration energy harvesting using different energy harvesting methodologies, further improvement in terms of design and materials is sought.

Electrostatic, electromagnetic, and piezoelectric are the most commonly pursued energy harvesting mechanisms. A generic spring-mass-damper model was presented by Williams, where the electrical energy harvested is equivalent to the energy dissipated in the electrical damper [1]. Electrostatic energy harvesting devices are typically classified into three

different types: in-plane overlap varying, in-plane gap closing, and out-of-plane gap closing [2]. Meninger and colleagues generated $8 \mu\text{W}$ at 2.5 kHz from an in-plane overlap electrostatic generator [3]. Other work includes the development of a device with high electrical damping, found to have an efficiency of 60% [4], and non-resonant electrostatic harvesting devices [5, 6]. In addition to the electrostatic technique, devices based on electromagnetic energy harvesting are also being pursued. An electromagnetic energy harvesting device that employs two and four magnet configuration has been developed to harvest energy from car vibrations [7]. Saha *et al* have presented modelling and optimization of an electromagnetic-based generator for generating power from ambient vibrations [8]. A 0.1 cm^3 volume device was shown to generate 30% of the power available from low level ambient vibrations [9]. Other work in this area includes a novel approach of up-converting the frequency to achieve higher power output from low frequency sources [10].

However, the piezoelectric energy harvesting technique is being widely pursued in the area of vibration energy harvesting because of its simplicity in design and ability to have higher power densities. Comprehensive reviews of power harvesting research using piezoelectric materials by Sodano *et al* are available in the literature [11, 12]. Sodano *et al* have developed a model to estimate the charge generated from piezoelectric energy harvesting technique [13], and have compared the performance of three different commercially available piezoelectric devices [14]. Roundy has proposed that the piezoelectric energy harvesting technique is the most efficient as it enables the highest energy density [15, 16], and proposed a cantilever design to power a Pico radio [16]. Other designs include a non-uniform thickness piezoelectric cantilever beam [17], and a clamped circular plate geometry [18, 19]. Recently MEMS scale energy harvesting devices have also been developed [20–22]. In addition to the common techniques described above, the magnetostrictive technique has also been adopted for energy harvesting [23, 24].

Apart from designing and developing an efficient conversion mechanism, a major challenge in vibration energy harvesting is the need to have a technique to tune the resonant frequency of the harvesting device to match the source frequency. Leland *et al* have proposed the application of an axial compressive load for tuning a simply supported vibration structure [25]. Challa *et al* have recently presented a magnetic force resonance frequency tuning technique that provides a 40% bandwidth and allows the device to be tuned to both lower and higher source frequencies [26].

In this paper, a coupled energy harvesting technique is presented. Coupling of energy harvesting mechanisms is used to increase the energy output in comparison to the performance of the stand-alone devices. (Throughout this paper ‘stand-alone’ refers to a device using only one energy harvesting mechanism, optimized to provide maximum power output for the given vibration source.) The organization of the paper is as follows: first, the theoretical background of the coupled technique is presented in terms of the effect of damping on the power output of a generic device. The coupled technique is then illustrated through a coupled piezoelectric–electromagnetic energy harvesting device because of its

simplicity in design and development. Whereas earlier work of the authors demonstrated the incorporation of variable magnetic stiffness into the system as a means to enable frequency tuning of a cantilever-based piezoelectric device [26], in the current work the coupling of piezoelectric and electromagnetic techniques is pursued as a means to optimize the overall efficiency of the coupled device from the perspective of electrical damping. The experimental techniques for determining the power outputs and the damping parameters for the stand-alone and coupled prototype devices are then discussed. Further, additional experimental validation is performed on a coupled device that employs the d_{33} piezoelectric mode cantilever beam, which also shows a large increase in power output through the coupling technique.

2. Generic coupled vibration energy harvesting model

In the following sections, a theoretical power output model is presented for the generic case of two independent energy harvesting techniques which are coupled for increased efficiency. The increase in efficiency is obtained by matching the total electrical damping to the mechanical damping in the system. The effect of total damping and ratio of electrical to mechanical damping on the power output of the harvesting device are also discussed.

2.1. Lumped model of a generic coupled vibration energy harvesting device

In this section the theoretical modelling and analysis of a generic (geometry and structure independent) coupled energy harvesting device is discussed. A simple single degree-of-freedom (lumped parameter) model is chosen here for simplicity (the limitations of such an approach for piezoelectric energy harvesting has recently been discussed in the literature [27, 28]). A coupled device is one that employs two (or more) separate energy conversion techniques for maximizing the power output of the device. It is to be noted that when coupled each technique alters the vibration response of the device, which in turn alters the power output obtained from each individual energy harvesting technique. In general, any generic energy harvesting device can be represented as a spring-mass-damper system, consisting of a mechanical damper (which accounts for the energy losses due to structural and viscous damping), and at least one electrical damper (to account for the energy harvested through an energy conversion mechanism) [1]. Since a coupled harvesting approach consists of two (or more) energy conversion mechanisms, an additional electrical damper is introduced into the system as shown in figure 1, where b_m , b_{e1} , and b_{e2} are mechanical and electrical damping constants, respectively. Here the vibrating structure is represented as a spring with a stiffness K_{struc} and mass m_{struc} . A source base vibration of $y(t) = Y \sin \omega_s t$ (where Y and ω_s are source vibration amplitude and frequency, respectively) generates a relative deflection $z(t)$ in the vibrating structure.

As shown by Williams [1], the power output from the coupled device (with two electrical dampers) can be written

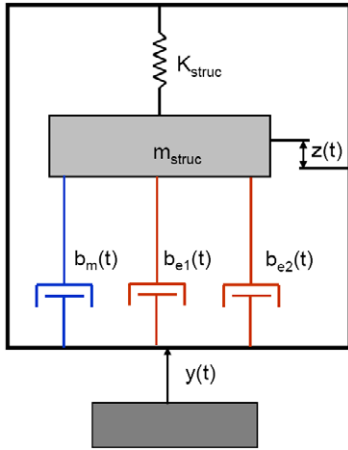


Figure 1. Lumped model of the coupled energy harvesting technique.

as

$$P_{\text{coupled}} = \frac{m_{\text{struc}} \left(\frac{\omega_s}{\omega_{\text{struc}}} \right)^3 \omega_s^3 (\zeta_{e1} + \zeta_{e2}) Y^2}{\left[\left[1 - \left(\frac{\omega_s}{\omega_{\text{struc}}} \right)^2 \right]^2 + 2\zeta_t \frac{\omega_s}{\omega_{\text{struc}}} \right]^2} \quad (1)$$

where ζ_t is the total damping ratio ($\zeta_t = \zeta_m + \zeta_{e1} + \zeta_{e2}$), $\zeta_m = b_m/2m_{\text{struc}}\omega_{\text{struc}}$ and $\zeta_{ei} = b_{ei}/2m_{\text{struc}}\omega_{\text{struc}}$ are the mechanical and electrical damping ratios of each energy harvesting technique in the system, and ω_{struc} is the undamped natural frequency of the vibrating structure,

$$\omega_{\text{struc}} = \sqrt{\frac{K_{\text{struc}}}{m_{\text{struc}}}}. \quad (2)$$

From equation (1), the power output of the device when in resonance ($\omega_s = \omega_{\text{struc}}$) can be simplified as

$$P_{\text{coupled}} = \frac{m_{\text{struc}} \omega_{\text{struc}}^3 (\zeta_{e1} + \zeta_{e2}) Y^2}{4\zeta_t^2}. \quad (3)$$

From equation (3), it is clear that when the device is in resonance, the output power generated by the device

is dependent on the resonance frequency, effective mass, amplitude of the source vibration, and damping components in the system. As the vibration amplitude and frequency are prescribed by the environmental source and thus not design variables, the vibrating structure has to be designed to match the source frequency. For a given vibrating structure the effective mass can be optimized based on the yield strength of the structure and the desired natural frequency. The other parameter that can be optimized in equation (3) to maximize the power output of the device are the damping parameters in the system.

2.2. Effect of damping on the power output of a generic coupled energy harvesting device

From equation (3), it is evident that the total power output is a function of both the electrical damping induced by the energy harvesting techniques as well as the total damping in the system. The ratio of the power output to the maximum possible (peak) power output is plotted in figure 2(a) as a function of the ratio of the electrical damping ($\zeta_e = \zeta_{e1} + \zeta_{e2}$) to mechanical damping ζ_m in the system using equation (3). It is evident from figure 2(a) that peak power is obtained if the electrical damping matches the mechanical damping. In addition, when the electrical damping is less than the mechanical damping in the system, the incorporation of additional electrical damping, via coupling with an additional energy harvesting mechanism, would result in an increase in the total power output. (As discussed by Stephen [29], the mechanical damping must be greater than zero for a realistic system to prevent unbounded vibration amplitude at resonance.) Figure 2(b) illustrates the total power output of the device with respect to the ratio of device frequency to source frequency at various damping values in the system for the case where the electrical damping matches the mechanical damping of the system (arbitrarily normalized with respect to a peak power that would be obtained for a theoretical mechanical damping of 0.001). With the introduction of an additional electrical damping component, the total damping in the system increases, thereby reducing the power output as can be seen in figure 2(b). However, as will

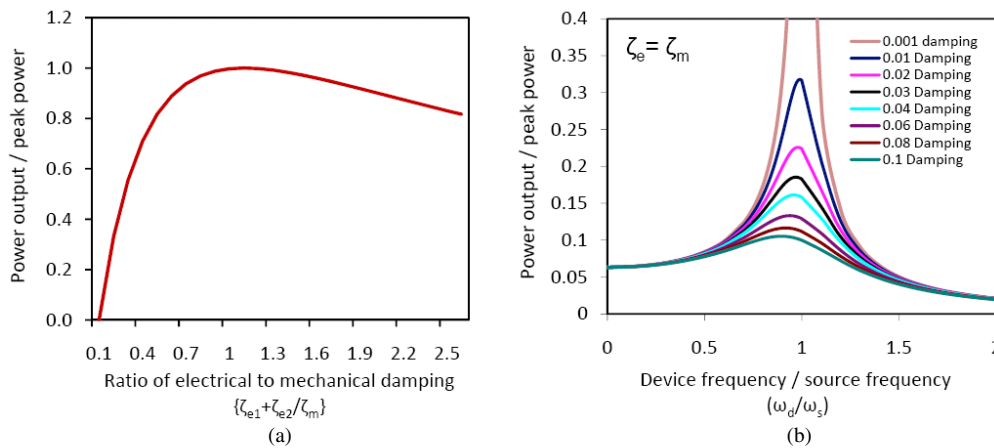


Figure 2. Ratio of power output to peak power as a function of (a) the electrical-to-mechanical damping ratio, (b) the ratio of device frequency to source frequency (arbitrarily defined for a total damping of 0.001) for the case where the electrical damping equals the mechanical damping in the system.

be shown experimentally in section 5, despite the decrease in power output with total damping, the total power output of the coupled device (now the sum of the power output from two energy harvesting techniques) can be increased by increasing the electrical damping to more closely match the mechanical damping in the system. Alternatively, for the case where the $\zeta_e < \zeta_m$, figure 2(b) suggests that one could also seek to decrease the mechanical damping such that $\zeta_e = \zeta_m$ is satisfied, which will also result in an increase in power output.

3. Coupled piezoelectric–electromagnetic energy harvesting technique

While the discussion in section 2 described a generic coupled technique, for simplicity the remainder of this work will focus on a coupled piezoelectric–electromagnetic energy harvesting technique that utilizes a cantilever beam design as the vibrating structure. A discussion of the damping contributions from the piezoelectric and electromagnetic techniques is presented with a theoretical model for estimating the total power output of the coupled energy harvesting device. Note that this coupled model could also be readily adapted if alternative energy harvesting techniques (electrostatic, magnetostrictive, etc) were used.

Here, a piezoelectric cantilever beam with a permanent magnet as its tip mass is employed. The permanent magnet allows one to couple the electromagnetic technique to the piezoelectric technique by placing a coil in the axis of motion of the magnet as shown in figure 3. The total energy harvested from such a coupled technique is the sum of the energies generated from the piezoelectric and electromagnetic mechanisms. By coupling the techniques, the total electrical damping in the system is now the sum of the piezoelectric and electromagnetic damping contributions; each also contributes to the total damping in the system. The increase in total damping reduces the vibration amplitude of the structure (in this case the cantilever beam), thereby reducing the stresses and the corresponding power output from the piezoelectric technique. Thus from a design perspective the energy harvested from the electromagnetic technique must be greater than the decrease in the energy from the piezoelectric technique to result in a net increase in power output of the coupled device. It is to be noted that the coupled device would have higher power output only for the case when electrical damping from piezoelectric technique is less than the mechanical damping in the system as explained in section 2.2.

3.1. Power output from stand-alone piezoelectric energy harvesting technique

The power generated from the stand-alone piezoelectric harvesting technique P_p irrespective of the geometry (cantilever, fixed–fixed, membrane, etc) can be written as

$$P_p = \frac{V_o^2 R_{Lp}}{(R_S + R_{Lp})^2} \quad (4)$$

where V_o is the generated open voltage from the piezoelectric beam. When the applied load resistance R_{Lp} (the external

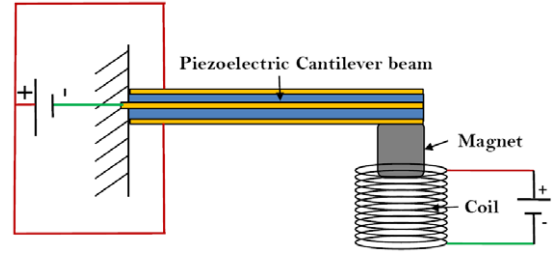


Figure 3. Schematic of a coupled piezoelectric–electromagnetic energy harvesting device (here a cantilever beam is used as the vibrating structure).

resistive load at which the output power is harvested) is equal to the source resistance R_S (also referred to as the source impedance), a condition referred to as impedance matching, maximum piezoelectric power output is obtained and is given as

$$P_p = \frac{V_o^2}{4R_S}. \quad (5)$$

(Experimentally, the piezoelectric power output P_p is equal to V_{Lp}^2/R_{Lp} , where V_{Lp} is the measured voltage at applied load resistance, R_{Lp}). The open voltage V_o generated depends on the stress developed in the structure σ_{struc} and the material properties of the piezoelectric material, such that

$$V_o = \frac{-d_{3i} t_p \sigma_{struc}}{\epsilon} \quad (6)$$

where t_p is the thickness of the piezoelectric layer, $-d_{3i}$ is the piezoelectric strain constant (where i is either 1 or 3 depending on whether the piezoelectric mode is d_{31} or d_{33}), and ϵ is the dielectric constant of the piezoelectric material. By inserting equation (6) into (5), the piezoelectric power output can be written as

$$P_p = \frac{\left(\frac{-d_{3i} t_p \sigma_{struc}}{\epsilon}\right)^2}{4R_S}. \quad (7)$$

For the specific case of a cantilever beam structure, the average stress generated σ_{struc} can be written as (see appendix)

$$\sigma_{struc} = \frac{3Ec}{4L_{eff}^2} \frac{a}{\zeta_t \omega_{struc}^2} \quad (8)$$

where E is the modulus of the composite beam (including the piezoelectric and electrode layers), L_{eff} is the length of the beam, and c is the distance of the electrode layer from the neutral axis. Substituting (8) into (7), the corresponding power output from the piezoelectric mechanism can be written as

$$P_p = \frac{9}{64R_S} \left(\frac{-d_{3i} t_p E c a}{\epsilon L_{eff}^2 \zeta_t \omega_{struc}^2}\right)^2. \quad (9)$$

From equation (9) it is clear that the power output of the piezoelectric cantilever decreases with an increase in total damping of the system.

3.2. Power output from stand-alone electromagnetic energy harvesting technique

When a magnet attached to the cantilever tip passes through the fixed coil, a current is produced in the coil due to Faraday's law. The rate at which the current produced corresponds to the power output of the electromagnetic energy harvesting device, P_{em} , is given as [9]

$$P_{em} = \frac{m_{struc}\omega_{struc}^3(\zeta_{em})Y^2}{4\zeta_t^2} \quad (10)$$

where ζ_{em} and ζ_t are the electromagnetic and total damping in the system. The electromagnetic damping can be derived as given in [30] as

$$\zeta_{em} = \frac{(NBl)^2}{2m_{struc}\omega_{struc}(R_{Lem} + R_{Coil})} \quad (11)$$

where N , l and B correspond to the number of turns, length of the coil, and the magnetic flux density. For peak power output from the electromagnetic technique one must match the load resistance R_{Lem} to the coil resistance R_{Coil} [31], and thus substituting equation (11) into (10) yields

$$P_{em} = \frac{(NBl\omega_{struc}Y)^2}{16\zeta_t^2 R_{Coil}}. \quad (12)$$

The magnetic flux density B of a cylindrical magnet at a distance d along the normal axis of the cylinder can be written as

$$B = \frac{B_r}{2} \left[\frac{d + h_m}{\sqrt{(d + h_m)^2 + r^2}} - \frac{d}{\sqrt{d^2 + r^2}} \right] \quad (13)$$

where B_r is the residual magnetic flux density (a physical property of the magnet), h_m is the height of the magnet, and r is the radius of the magnet. Experimentally (see section 4) it will prove useful to write equation (12) in terms of the amplitude of the source acceleration (rather than the amplitude of beam vibration) using the relationship $a = Y\omega_{beam}^2$, such that

$$P_{em} = \frac{(NlBa)^2}{16\zeta_t^2\omega_{struc}^2 R_{Coil}}. \quad (14)$$

It is clear from equation (14) that the power output from the electromagnetic approach is also dependent on the total damping of the system.

3.3. Power output from coupled energy harvesting technique

For a coupled device assumed to be in resonance, the total power output is the sum of the power generated from the piezoelectric and electromagnetic harvesting techniques. However, it is critical to note that this total power output is *not equal* to the sum of the individual stand-alone power outputs generated from the piezoelectric and electromagnetic techniques, but is now a function of the total damping in the system as a result of coupling, such that

$$P_{coupled} = P_p + P_{em} = \frac{1}{4R_s} \left(\frac{-d_{3i}t_p\sigma_{coupled}}{\varepsilon} \right)^2 + \frac{(NlBa)^2}{16\zeta_t^2\omega_{struc}^2 R_{Coil}} \quad (15)$$

where $\sigma_{coupled}$ is the stress in the piezoelectric beam in the coupled device, which is a function of the vibration amplitude of the beam and thus depends on the total damping in the system. For a harvesting device with a cantilever beam geometry in resonance at the source frequency, the coupled power output can be given by substituting equation (9) into equation (15). Note again that the piezoelectric power output decreases with coupling of the energy harvesting techniques, as with the addition of the electromagnetic technique the total damping in the system increases. Similarly a decrease in electromagnetic power output is obtained when a piezoelectric technique is coupled to an existing electromagnetic technique. As discussed in section 2.2, the total power output of the coupled device would be greater than that obtained from the stand-alone piezoelectric device only when the sum of the electrical damping from both piezoelectric and electromagnetic techniques does not exceed the mechanical damping in the system.

3.4. Damping from the piezoelectric and electromagnetic energy harvesting techniques

Clearly, to maximize the power output of the device, the electrical damping contributed by the energy harvesting techniques should match the mechanical damping in the system. Hence it is important to understand how one can alter the electrical damping from the energy harvesting techniques. In the discussion below, it is assumed that the vibrating structure is in resonance with the forcing frequency.

If only a piezoelectric energy harvesting mechanism is considered, from equation (3) the power at which the energy is dissipated in the damper is equal to the power output of the energy harvesting cantilever beam (see equation (9)). By equating these powers the piezoelectric damping ratio for the case of a cantilever beam structure can be written as

$$\zeta_p = \frac{3}{16R_{Lp}} \left(\frac{d_{3i}^2 t_p^2 E_{struc} c^2}{I \varepsilon_p^2 L_{eff} \omega_{struc}} \right) \quad (16)$$

where I is the moment of inertia of the beam. Since the impedance of the piezoelectric beam is constant for a given geometry and structure (frequency), the optimal value of piezoelectric damping will also remain constant. For a given piezoelectric material and geometry, quantities such as Young's modulus, piezoelectric strain coefficient, dielectric constant, capacitance, and natural frequency are constant, leaving the applied load resistance as the only parameter that can alter the piezoelectric damping as given in equation (16). This is illustrated in figure 4(a) using the material parameters and geometry given in table 1. The figure shows that the induced piezoelectric damping increases with the applied load resistance; for peak power output, this applied load resistance should match the impedance of the piezoelectric beam (also known as the source resistance; see equation (4)). Note that even though the piezoelectric damping increases with load resistance, the power extracted would decrease when the load resistance becomes greater than the impedance in the beam. Hence in terms of electrical optimization, the load resistance is limited by the impedance of the beam.

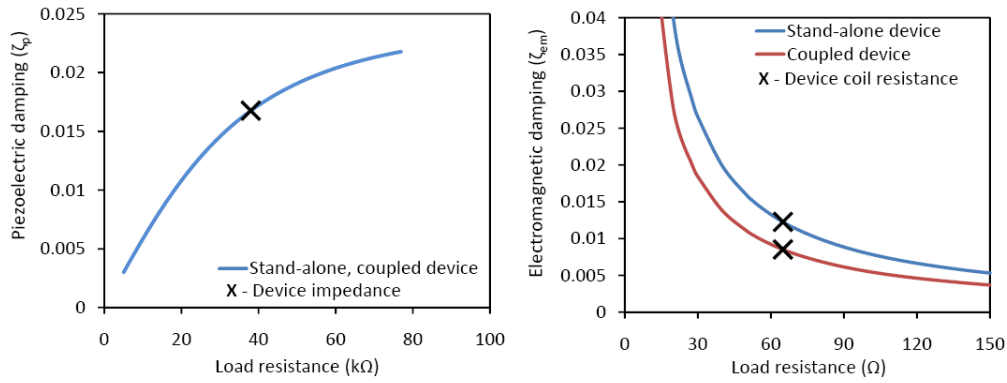


Figure 4. Theoretical values of (left) piezoelectric damping with respect to load resistance, and (right) electromagnetic damping with respect to load resistance for two different setups (stand-alone, coupled). Parameters used to plot these curve are given in table 1. Marked in each plot is the theoretically determined damping value when the conditions of impedance matching are satisfied.

Table 1. Parameter descriptions and their values (Device 1).

Symbol	Description	Units	
B_r	Residual flux density	1.1	T
d	Distance of the coil from the magnet (stand-alone device)	1.7	mm
	Distance of the coil from the magnet (coupled device)	2	mm
A	Area of the magnet	25.1	mm ²
h_m	Height of the magnet	2.95	mm
R	Radius of the magnet	4	mm
μ_o	Permeability of intervening medium	1.256×10^{-6}	H m ⁻¹
m_t	Mass of the magnet	31	g
E	Young's modulus	3.81×10^{10}	GPa
I	Moment of inertia	0.36	mm ⁴
L	Length of the beam	36	mm
b	Width of the beam	20	mm
h	Thickness of the beam	0.6	mm
M_{struc}	Effective mass of the beam with tip mass	44.3	g
$-d_{31}$	Piezoelectric strain coefficient of the material	-1.75×10^{-10}	C N ⁻¹
E	Dielectric constant	1.55×10^{-8}	F m ⁻¹
C_p	Capacitance	1.7×10^{-7}	F
t_p	Thickness of piezoelectric layer	0.16	mm

For simplicity, the piezoelectric damping in our single degree-of-freedom system is considered above to be linear viscous. More rigorous models which better incorporate the electrical and mechanical coupling of piezoelectric energy harvesters have recently been described in the literature [27, 28]. Such models are particularly necessary when trying to model the complete coupled system dynamics at arbitrary load resistances and non-resonant frequencies. (Because the optimal piezoelectric load resistance and resonant frequencies are determined experimentally in section 5, the simplified models used here are assumed to be sufficient for purposes of this work.)

Similarly, the electrical damping from the electromagnetic energy harvesting ζ_{em} was given in equation (11) and is plotted in figure 4(b), which shows that the damping decreases with increase in load resistance. Hence the load resistance has

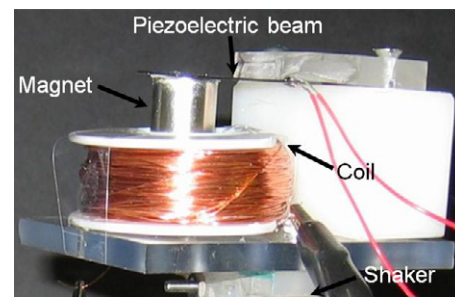


Figure 5. Photograph of the coupled electromagnetic–piezoelectric energy harvesting device (Device 1).

to be minimal to have high electrical damping; however, for obtaining peak power output the applied load resistance should match the coil resistance [31]. Other methods to increase the electromagnetic damping are to employ a high residual magnetic flux density magnet or to place the coil in the closest proximity of the magnet, which are limited by the material property and the feasible distance, respectively. For the case of matching load resistance to coil resistance, the electrical damping ratio was found to be 0.012 for the stand-alone device and 0.008 for the coupled energy harvesting device setup, respectively. These different electromagnetic damping ratios are achieved by placing the coil at different distances (1.7 and 2 mm) from the magnet to change the magnetic flux density (see equation (13)).

4. Experimental method

To illustrate the design of a coupled energy harvesting technique, a piezoelectric–electromagnetic device was fabricated consisting of a stripe actuator (APC International, Ltd) used as the vibrating cantilever beam structure (this will be referred as Device 1 from this point forward). The piezoelectric cantilever beam is a bimorph with two piezoelectric layers sandwiched between three electrodes in a parallel configuration. An Nd-FeB magnet (K&J Magnetics, Inc) with a residual magnetic flux density of 1.1 T is attached to the piezoelectric cantilever beam as a tip mass. A copper coil is placed in the axis of the motion of the magnet as shown in figure 5. The entire device is

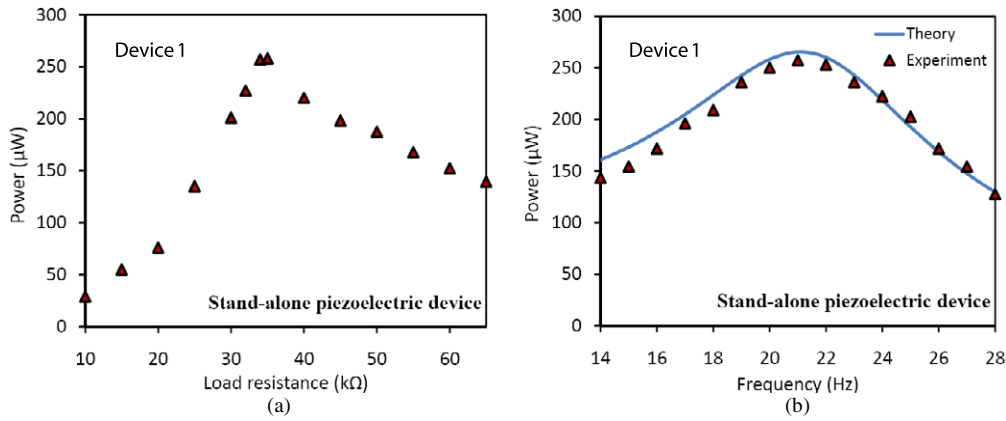


Figure 6. Power output of the stand-alone (a) piezoelectric energy harvesting device (Device 1), (b) electromagnetic energy harvesting device (Device 1).

mounted on a shaker table (Bruel and Kjaer) that is connected to a function generator (HP 4120 series) through a power amplifier (Bruel and Kjaer). The function generator and power amplifier are used to provide the desired source excitation to the system. The voltage that is generated in the piezoelectric beam is captured by means of lead wires soldered to the electrodes. The lead wires are in turn connected across a variable resistor that allows altering the load resistance to obtain peak power output. Similarly, the current generated in the coil due to electromagnetic power is captured as a voltage across another variable resistor.

For comparison with the power output from the coupled device, the stand-alone techniques are also separately implemented and individually optimized for peak power output. For the stand-alone piezoelectric technique, the electromagnetic energy harvesting coil is removed so that there is no damping from the electromagnetic technique. The mechanical damping in the system is determined by employing a no load condition ($R_{Lp} = 0$), which implies that no energy is dissipated through the piezoelectric technique. The damping value is obtained by performing a flick test (flicking the cantilever at the tip and monitoring the decay of the vibration amplitude over time), through which an amplitude decay plot is obtained and the corresponding damping is determined using the relationship

$$\zeta = \frac{1}{2\pi} \ln\left(\frac{a_1}{a_2}\right) \quad (17)$$

where a_1 and a_2 are consecutive peak amplitudes.

As explained in section 3.2, to obtain the peak power output of the piezoelectric energy harvesting device, the load resistance has to match the beam impedance. Experimentally the beam impedance (optimal load resistance) value is determined by performing a load resistance sweep test while monitoring the power output of the piezoelectric beam; at peak power output the corresponding load resistance value is the impedance in the beam. With this load condition, an amplitude decay plot is obtained through the flick test and the corresponding damping value is determined. The damping value obtained in this case is now the sum of the mechanical and the piezoelectric (electrical) damping of the stand-alone

piezoelectric device; the difference between this damping value and the damping value with no load (purely mechanical damping) yields the value of the piezoelectric damping in the system.

To characterize the stand-alone electromagnetic energy harvesting device, the lead wires that were connected to the piezoelectric beam are disconnected such that no energy is dissipated through the piezoelectric mechanism. In this case the piezoelectric cantilever beam simply acts as a vibrating cantilever with losses only due to mechanical damping in the structure. Once the electromagnetic coil is in place and properly wired the electrical damping in the system is purely electromagnetic. The electromagnetic electrical damping in this case is given by the difference in damping values obtained by employing the optimal load condition ($R_{Lem} = R_C$) and the mechanical damping of the beam at no load condition ($R_{Lp} = 0$).

5. Results and discussion

5.1. Power output from stand-alone piezoelectric and electromagnetic devices (Device 1)

The power output from the stand-alone piezoelectric and electromagnetic devices (Device 1) is determined along with the mechanical and electrical damping parameters in the system. The natural frequency of the piezoelectric cantilever beam with tip mass was determined to be 21.6 Hz. The optimal load resistance for the piezoelectric device is determined experimentally to be 35 k Ω (as explained in section 4); at this condition a peak power output of 257 μW is obtained as shown in figure 6(a). The associated mechanical and piezoelectric damping values at $R_{Lp} = 0$ and 35 k Ω are determined experimentally as described in section 4 using the flick test. The mechanical damping is found to be 0.023 and total damping to be 0.038, which yields a piezoelectric damping of 0.015. Since the piezoelectric damping is less than the mechanical damping in the system, a further increase in electrical damping (to match the mechanical damping in the system) is sought to obtain the maximum possible power output. Using the obtained optimal load resistance value of 35 k Ω , the experimental power output is plotted with

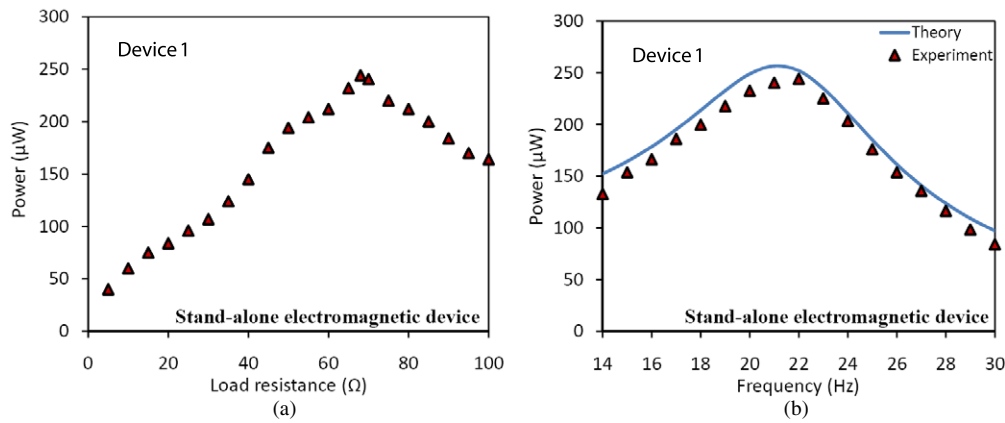


Figure 7. Power output of the stand-alone electromagnetic energy harvesting device (Device 1) versus (a) load resistance and (b) frequency.

respect to source frequency in figure 6(b) and compared to the theoretical power output of the stand-alone piezoelectric device using equation (9) with the experimentally determined damping values.

Similarly, the stand-alone electromagnetic device is configured as described in section 4, and the corresponding power output, optimal load resistance and electromagnetic damping values are determined. At an optimal load of 68 Ω , a peak power output of 244 μW is obtained as shown in figure 7(a), resulting in an electromagnetic damping ratio of 0.012. Again this electromagnetic damping value is less than the earlier determined mechanical damping in the beam (0.023), suggesting an increase in electrical damping through coupling is desired. It is to be noted that the power output of the stand-alone electromagnetic device could be increased by using a cantilever beam with a mechanical damping value lower than that of the piezoelectric cantilever beam used here. However, since the goal of this work is to ultimately maximize the power output of the piezoelectric-based device through coupling with an electromagnetic technique, the same piezoelectric beam is employed here. Figure 7(b) shows the power output of the stand-alone electromagnetic device performance as a function of source frequency at the optimal load resistance determined in figure 7(a).

5.2. Coupled electromagnetic–piezoelectric energy harvesting device power output (Device 1)

The coupled piezoelectric–electromagnetic device (Device 1) was built and tested as described in section 4. Since the sum of the electrical damping from stand-alone piezoelectric (0.015) and electromagnetic techniques (0.012) of the device is greater than the mechanical damping in the system, the coil is relocated from 1.7 to 2 mm from the magnet, which alters the magnetic flux density such that the resulting value of electromagnetic damping is 0.008, such that the total electrical damping now matches the mechanical damping in the system (0.023). Using the optimal load resistance conditions determined from the stand-alone techniques, a total power output of 332 μW is obtained at the resonance frequency of 21.6 Hz as shown in figure 8. The obtained experimental power output compares favourably with the theoretical model

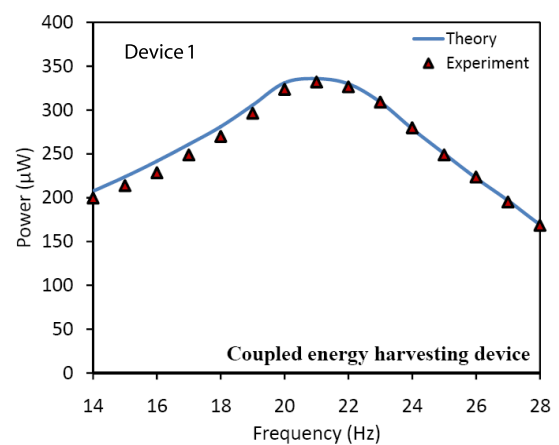


Figure 8. Power output of the coupled piezoelectric–electromagnetic energy harvesting device (Device 1) versus the source vibration frequency.

obtained using the experimentally determined damping values (see equation (15)). The contribution of piezoelectric and electromagnetic power outputs towards the total power of the coupled device are 187 μW and 145 μW , respectively. As expected, the individual power outputs from each of the energy harvesting techniques when coupled were reduced because of the increase in total damping in the system. Hence the power output of the coupled device is *not* equal to the sum of the stand-alone power outputs from the optimized techniques, but rather is a function of the change in total damping in the coupled system.

5.3. Additional device experimental validation (Device 2)

An additional device (referred as Device 2) was built to validate the proposed coupled energy harvesting approach. The built device consists of a piezoelectric fibre composite (Advanced Cerametrics, Lambertville, NJ) cantilever which operates in d_{33} mode (stress and electric charge are in the same direction). An NdFeB magnet is again used as both the tip mass and the magnet for the electromagnetic harvesting approach. The experimental procedure described above is carried out to determine the damping values and power outputs

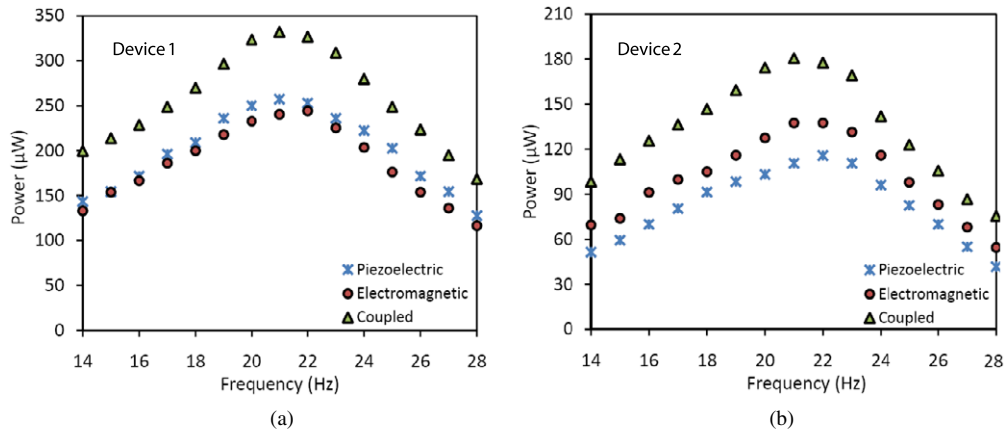


Figure 9. Comparison of power output from the coupled and stand-alone energy harvesting techniques (a) Device 1 (b) Device 2. (Note: the power output from the coupled device is not equal to the sum of the stand-alone piezoelectric and electromagnetic techniques due to changes in total damping of the system).

Table 2. Experimental damping and total power output values of Device 1 and Device 2.

Parameter	Stand-alone piezoelectric		Stand-alone electromagnetic		Coupled	
	Dev. 1	Dev. 2	Dev. 1	Dev. 2	Dev. 1	Dev. 2
Mechanical damping	0.023	0.027	0.023	0.027	0.023	0.027
Piezoelectric damping	0.015	0.014	—	—	0.015	0.014
Electromagnetic damping	—	—	0.012	0.012	0.008	0.012
Ratio of electrical to mechanical damping	0.652	0.519	0.522	0.565	1	0.963
Total damping	0.038	0.042	0.035	0.04	0.046	0.053
Piezoelectric power (μW)	257	110	—	—	187	86
Electromagnetic power (μW)	—	—	244	137	145	96
Total power output (μW)	257	110	244	137	332	182
Increase in power output (%)	—	—	—	—	30	65.5
Power density ($1 \mu\text{W cm}^{-3}$)	9.1	2.2	6.9	2.4	9.5	3.2

of stand-alone piezoelectric and electromagnetic devices. The mechanical, piezoelectric and electromagnetic damping values are found to be 0.027, 0.014 (at its optimal load of 0.7 MΩ) and 0.012 (at its optimal load of 68 Ω), respectively, from their corresponding stand-alone devices for this setup. The peak power outputs from the stand-alone piezoelectric and electromagnetic devices of Device 2 are 110 and 137 μW, with the total power output of the coupled device found to be 182 μW.

5.4. Comparison and discussion of energy harvesting techniques

The two coupled devices (Device 1 and Device 2) are compared to their respective optimized, stand-alone piezoelectric and electromagnetic devices in figure 9, respectively, in terms of power output. The various damping values for the stand-alone configurations as well as the coupled devices are summarized in table 2. From figure 9(a) the total power output of the coupled technique of Device 1 is 332 μW, while the stand-alone piezoelectric power output is only 257 μW and the stand-alone electromagnetic power output is 244 μW. Here the piezoelectric and electromagnetic damping values of the stand-alone devices are 0.015 and 0.012, respectively, each of which

is less than the value of the mechanical damping in the system (0.023). Hence by coupling the two techniques to increase the electrical damping in the system (note here the magnetic flux density was altered by adjusting the distance between the magnet and the coil to reduce the electromagnetic damping to the desired value of 0.008), the electrical and mechanical damping are matched and an increase in the total power output of the coupled device is realized. Similarly from figure 9(b), the power output of the coupled technique of Device 2 is 182 μW as compared to the stand-alone power outputs of its corresponding piezoelectric and electromagnetic techniques of 110 μW and 137 μW, respectively. Here the piezoelectric and electromagnetic damping values of the stand-alone devices were 0.014 and 0.012, respectively, which when added together are very close to the mechanical damping value (0.027) of the system.

These results indicate that the coupled device has an improved power output over the stand-alone piezoelectric and electromagnetic techniques, due to the increase in electrical damping to match the mechanical damping in the system. This enhancement in the electrical damping of the coupled device resulted in an increase in power output by 30% and 65.5% for Device 1 and Device 2, respectively. With the increase in electrical damping, the total damping in the system

also increases, which decreases the corresponding power output contribution of the original energy harvesting technique. Hence an optimization has to be performed for maximizing the power output of the device with respect to the increase in the additional induced electrical damping (and the total damping) in the system.

One can also compare the device performance based on the power density. Based on the volumes occupied by each device, the corresponding power densities are listed in table 2. It is noteworthy to observe that while the output power was greater for the coupled device, the increase in power density is nominal due to the increase in volume of the coupled device. For applications where the design goal is to maximize the overall power density, the extra volume necessary to couple two individual energy harvesting techniques must be considered as an additional design variable.

For the case where only a stand-alone piezoelectric device is desired to achieve peak power, the electrical damping can be increased by employing higher piezoelectric strain coefficient (d_{3i}) materials (see equation (16)), which may be cost ineffective when compared to a coupled technique. Similarly, for the stand-alone electromagnetic technique, a more conductive coil and/or a higher magnetic flux density magnet can be employed to further enhance the electrical damping to achieve peak possible power. Alternatively, if the mechanical damping in the system can be reduced through design [10], the power output of the energy harvesting device would increase significantly. For example, in the case of coupled Device 1, if the mechanical damping could be decreased from 0.023 to 0.015 (which would match the electrical damping value of the stand-alone piezoelectric Device 1), one can again use equation (3) to show that the theoretical power output of the device in this case would be 412 μ W, resulting in an increase in power output by 60%.

6. Conclusions

A coupled energy harvesting approach is presented which emphasizes the importance of consideration of the damping parameters to obtain optimal power output. It is demonstrated that electrical damping can be increased to match the mechanical damping in the system through introduction of additional energy harvesting mechanisms within the design. To illustrate the coupled energy harvesting technique, two different coupled piezoelectric–electromagnetic devices were developed and tested. The total power output of the coupled devices was 332 μ W and 182 μ W for Device 1 and Device 2, respectively. Compared to 257 μ W and 110 μ W from the stand-alone piezoelectric devices, adding the electromagnetic harvesting mechanism in the system increased the total power output by 30% and 65.5%, respectively. The experimental results from the coupled devices show close agreement with a theoretical model developed for the coupled device which accounts for changes in the total system damping into power output calculations. Specifically, while the total electrical damping in the coupled system is the sum of the individual electrical damping components, the total power output of the coupled device is *not* simply the sum of the optimized, individual stand-alone energy harvesting techniques, as the

increase in total damping in the system reduces the vibration amplitude (and hence the strain) of the piezoelectric cantilever beam. By employing higher conversion coefficient materials, higher values of piezoelectric damping could be obtained to more closely match the mechanical damping in the system to improve the power output of the stand-alone (original) piezoelectric device, but in terms of cost effectiveness the use of a coupled device approach may be more desirable. Alternatively, another manner to significantly increase the power outputs from the energy harvesting techniques is by reducing the mechanical damping in the system. This work demonstrates a simple and effective way of increasing energy harvesting power output through coupling of energy harvesting techniques, while suggesting methods to further increase the power output of the device through materials and device design.

Appendix

Here one seeks to derive the average stress generated in the structure σ_{struc} at resonance as a function of the amplitude and frequency of the forcing vibration and the geometry and properties of the cantilever. First, one can calculate the tip force F_{tip} , which is the equivalent static force which, if applied at $x = L_{\text{eff}}$, would result in the same maximum deflection at the end of the beam as that when the beam is in resonance. This tip force can be determined based on the principle of force transmissibility [32] using equation (2) as

$$F_{\text{tip}} = \frac{F_{\text{dyn}}}{2\zeta_t} = \frac{m_{\text{struc}}a}{2\zeta_t} = \frac{\left(\frac{k}{\omega_{\text{struc}}^2}\right)a}{2\zeta_t} = \frac{ka}{2\zeta_t\omega_{\text{struc}}^2}. \quad (18)$$

To determine the average stress in the beam, one can now assume a static analysis where the stress in the beam is due to the application of a force of magnitude F_{tip} at a distance L_{eff} from the fixed end of the beam (to account for the finite width of the tip mass). From standard beam theory, the average stress on the surface of the cantilever beam can be calculated as

$$\sigma_{\text{struc}} = \frac{1}{L_{\text{eff}}} \int_0^{L_{\text{eff}}} \frac{Mc}{I} dx = \frac{F_{\text{tip}}L_{\text{eff}}c}{2I} \quad (19)$$

where the maximum moment $M = F_{\text{tip}}L_{\text{eff}}$, c is the distance from the neutral axis, and x is the distance from the tip of the cantilever beam in the axial direction. Substituting equation (18) into (19), and using the expression for the stiffness of a cantilever beam ($k = 3EI/L_{\text{eff}}^3$), the average stress in the cantilever beam at resonance can be written as

$$\sigma_{\text{struc}} = \frac{\left(\frac{ka}{2\zeta_t\omega_{\text{struc}}^2}\right)L_{\text{eff}}c}{2I} = \frac{kaL_{\text{eff}}c}{4\zeta_t\omega_{\text{struc}}^2I} = \frac{3Eac}{4L_{\text{eff}}^2\zeta_t\omega_{\text{struc}}^2}. \quad (20)$$

References

- [1] Williams C B and Yates R B 1996 Analysis of a micro-electric generator for microsystems *Sensors Actuators A* **52** 8–11
- [2] Roundy S, Wright P K and Rabaey J 2003 A study of low level vibrations as a power source for wireless sensor nodes *Comput. Commun.* **26** 1131–44

- [3] Meninger S, Mur-Miranda J O, Amirtharajah R, Chandrakasan A P and Lang J H 2001 Vibration-to-electric energy conversion *IEEE Trans. Very Large Scale Integr. (VLSI) Syst.* **9** 64
- [4] Despesse G, Chaillout J J, Jager T, Léger J M, Vassilev A, Basrour S and Charlot B 2005 High damping electrostatic system for vibration energy scavenging *Joint sOc-EUSAI Conf.* pp 1–6
- [5] Mitcheson P D, Miao P, Stark B H, Yeatman E M, Holmes A S and Green T C 2004 MEMS electrostatic micropower generator for low frequency operation *Sensors Actuators A* **115** 523–9
- [6] Miao P, Holmes A S, Yeatman E M and Green T C 2004 Micro-machined variable capacitors for power generation *Electrostatics Conf.* pp 53–8
- [7] Glynn-Jones P, Tudor M J, Beeby S P and White N M 2004 An electromagnetic, vibration-powered generator for intelligent sensor systems *Sensors Actuators A* **110** 344–9
- [8] Saha C R, O'Donnell T, Loder H, Beeby S and Tudor J 2006 Optimization of an electromagnetic energy harvesting device *IEEE Trans. Magn.* **42** 3509
- [9] Beeby S P, Torah R N, Tudor M J, Glynn-Jones P, O'Donnell T, Saha C R and Roy S 2007 A micro electromagnetic generator for vibration energy harvesting *J. Micromech. Microeng.* **17** 1257
- [10] Kulah H and Najafi K 2004 An electromagnetic micro power generator for low-frequency environmental vibrations *MEMS: IEEE Int. Conf. on Micro Electro Mechanical Systems* pp 237–40
- [11] Anton S R and Sodano H A 2007 A review of power harvesting using piezoelectric materials (2003–2006) *Smart Mater. Struct.* **16** R1–21
- [12] Sodano H A, Inman D J and Park G 2004 A review of power harvesting from vibration using piezoelectric materials *Shock Vib. Dig.* **36** 197
- [13] Sodano H A, Park G and Inman D J 2004 Estimation of electric charge output for piezoelectric energy harvesting *Strain* **40** 49–58
- [14] Sodano H A, Inman D J and Park G 2005 Comparison of piezoelectric energy harvesting devices for recharging batteries *J. Intell. Mater. Syst. Struct.* **16** 799
- [15] Roundy S and Wright P K 2004 A piezoelectric vibration based generator for wireless electronics *Smart Mater. Struct.* **13** 1131–42
- [16] Roundy S, Leland E S, Baker J, Carleton E, Reilly E, Lai E, Otis B, Rabaey J M, Wright P K and Sundararajan V 2005 Improving power output for vibration-based energy scavengers *IEEE Pervasive Comput.* **4** 28
- [17] Gao R X and Cui Y 2005 Vibration-based energy extraction for sensor powering: design, analysis, and experimental evaluation *Proc. SPIE* **5765** 794–801
- [18] Kim S, Clark W W and Wang Q-M 2005 Piezoelectric energy harvesting with a clamped circular plate: experimental study *J. Intell. Mater. Syst. Struct.* **16** 855–63
- [19] Kim S, Clark W W and Wang Q M 2005 Piezoelectric energy harvesting with a clamped circular plate: analysis *J. Intell. Mater. Syst. Struct.* **16** 847
- [20] Fang H B, Liu J Q, Xu Z Y, Dong L, Wang L, Chen D, Cai B C and Liu Y 2006 Fabrication and performance of MEMS-based piezoelectric power generator for vibration energy harvesting *Microelectron. J.* **37** 1280
- [21] Jeon Y B, Sood R, Jeong J H and Kim S G 2005 MEMS power generator with transverse mode thin film PZT *Sensors Actuators A* **122** 16–22
- [22] Shen D, Park J H, Ajitsaria J, Choe S Y, Wickle H C and Kim D J 2008 The design, fabrication and evaluation of a MEMS PZT cantilever with an integrated Si proof mass for vibration energy harvesting *J. Micromech. Microeng.* **18** 055017
- [23] Huang J, O'Handley R C and Bono D 2003 New high-sensitivity hybrid magnetostrictive/electroactive magnetic field sensors *Proc. SPIE* **5050** 229–37
- [24] Wang L and Yuan F G 2008 Vibration energy harvesting by magnetostrictive material *Smart Mater. Struct.* **17** 045009
- [25] Leland E S and Wright P K 2006 Resonance tuning of piezoelectric vibration energy scavenging generators using compressive axial preload *Smart Mater. Struct.* **15** 1413–20
- [26] Challa V R, Prasad M G, Shi Y and Fisher F T 2008 A vibration energy harvesting device with bidirectional resonance frequency tunability *Smart Mater. Struct.* **17** 015035
- [27] Erturk A and Inman D J 2008 Issues in mathematical modeling of piezoelectric energy harvesters *Smart Mater. Struct.* **17** 065016
- [28] Erturk A and Inman D J 2009 An experimentally validated bimorph cantilever model for piezoelectric energy harvesting from base excitations *Smart Mater. Struct.* **18** 025009
- [29] Stephen N G 2006 On energy harvesting from ambient vibration *J. Sound Vib.* **293** 409–25
- [30] El-hami M, Glynn-Jones P, White N M, Hill M, Beeby S, James E, Brown A D and Ross J N 2001 Design and fabrication of a new vibration-based electromechanical power generator *Sensors Actuators A* **92** 335–42
- [31] Kulkarni S, Koukharenko E, Torah R, Tudor J, Beeby S, O'Donnell T and Roy S 2008 Design, fabrication and test of integrated micro-scale vibration-based electromagnetic generator *Sensors Actuators A* **145/146** 336
- [32] Rao S S 2003 *Mechanical Vibrations* 4 edn (Upper Saddle River, New Jersey: Pearson)